Environmental Sciences Europe

RESEARCH

Open Access

Traceability tagging of volatile organic compound sources and their contributions to ozone formation in Suzhou using vehicle-based portable single-photon ionization mass spectrometry

Nazifi Sani Shuaibu[1†], Chenghua Qin[2*†], Fengjian Chu[1], Balarabe B. Ismail[3,4], Ammar Muhammad Ibrahim[5], Musbahu Garba Indabawa[5], S. A. A. Abdalmohammed[1], Gaosheng Zhao[6*] and Xiaozhi Wang[1*]

Abstract

Background In recent decades, there has been an increasing global preoccupation with atmospheric volatile organic compounds (VOCs). Given the significant impact of VOCs as pollutants and essential precursors of ozone (O_3) in urban and industrial areas, it is imperative to identify and quantify the sources of their emissions to facilitate the development and implementation of effective environmental control strategies.

Methods A mobile laboratory vehicle equipped with a single-photon ionization–time-of-flight mass spectrometer (SPI–TOFMS) and a navigation system was employed to establish the traceability of VOCs that contribute to the formation of ozone in Suzhou Industrial Park. The method exhibited a favorable detection limit of 0.090 ppbv, accompanied by a mass resolution of 1500 for the instrument and a correlation coefficient ≥ 0.990. A positive matrix factorization (PMF) model was utilized to determine the source appointment of the VOCs.

Results The study tentatively traced and identified the VOCs emissions source and their contribution to ozone formation in Suzhou. Using the PMF model, the sources of VOCs were profiled: three primary sources of VOCs were identified, namely, vehicular emissions, an industrial solvent, and biofuel combustion. Alkanes groups were found to be the most abundant VOCs species, accounting for 60% of the total VOCs, followed by aromatics and alkenes. Maximum incremental reactivity (MIR) quantifies the impact of photochemical reaction mechanism on the potential ozone formation.

Conclusions The findings of this study complement existing knowledge on the pollution status of atmospheric VOCs and highlight the correlation with ozone formation potential in Suzhou. The aforementioned sources were identified as the primary factors responsible for the pollution in Suzhou. The successful implementation of SPI–TOFMS

[†]Nazifi Sani Shuaibu and Chenghua Qin have contributed equally.

*Correspondence:
Chenghua Qin
qinch@cnemc.cn
Gaosheng Zhao
zgs571@shu.edu.cn
Xiaozhi Wang
xw224@zju.edu.cn
Full list of author information is available at the end of the article

has demonstrated a promising methodology that is well-suited for the real-time and online monitoring of VOCs in the atmosphere. In addition, a library for identifying VOC fingerprints from the same plant was established. This library serves as a comprehensive resource for establishing on-site VOC traceability, estimating source apportionment, and evaluating their impact on ozone formation.

Keywords Volatile organic compounds, Single-photon ionization, Time of flight, Mass spectrometry, Positive matrix factorization, VOC fingerprint

Background

The swift industrialization and urbanization in China have had significant implications for air quality and ecological stability and have led to notable challenges in environmental pollution [1–4]. The emission of volatile organic compounds (VOCs) into the atmosphere is undergoing rapid and exponential growth, emerging as a significant contributor to atmospheric pollution in China [5, 6]. In recent years, numerous research studies have been conducted throughout China to investigate the sources of VOCs emissions [7–9]. A significant proportion of VOCs consist of anthropogenic chemicals utilized in various manufacturing industries, such as paints, pharmaceuticals, and refrigerants. These compounds also originate from vehicle emissions [2, 3]. A notable proportion of VOCs are known for their unpleasant odors and present significant health hazards, leading to both acute and chronic illnesses, including respiratory diseases, premature mortality, lung cancer, and childhood asthma [10–16].

VOCs play a crucial role in atmospheric photochemical processes as key precursors to O_3 formation and other secondary organic aerosols [17]. Research investigating the correlation between O_3 and its precursors suggests that the formation of O_3 is limited in urban as well as industrial areas [18, 19]. Industrial-related emissions of VOCs, including benzene, toluene, and xylenes, prominently contribute to O_3 formation and the generation of secondary organic aerosols [20]. Tracing, identifying, and quantifying the sources of VOCs and other pollutant emissions are essential prerequisites for the analysis and development of strategies for controlling air pollution. Consequently, the development of an effective technique for managing the photochemical process, tracing VOCs emission sources, and quantifying their relationship with O_3 formation becomes imperative.

The reactivity-based approach, as proposed by [21], combines the positive matrix factorization (PMF) model with an observation-based model (OBM). This methodology was exclusively applied within the confines of non-urban interior zones. Since its establishment, the PMF model has been widely utilized for the purpose of identifying and quantifying VOCs in various regions across the globe [21–23].

In the present study, the PMF model is employed to delineate the primary sources of VOCs and to assess their contributions to the photochemical formation of O_3. The OBM, grounded in the carbon bond 4 mechanism, provides a valuable tool for scrutinizing the relation between O_3 and its precursors at specific geographical locations. These precursor compounds include VOCs, nitric oxide (NO_x), and carbon monoxide (CO) [23–25]. Unlike models that rely on emissions, the OBM incorporates observed ambient concentrations of O_3 and its precursors to simulate the photochemical formation and destruction of O_3. This approach helps to mitigate uncertainties associated with emission inventories [21, 26, 27].

However, some researchers tend to emphasize the contribution of specific VOCs to O_3 formation, often neglecting the influence of others. Such an approach may lead to inadequate analysis of the data. To overcome this, we adopt a comprehensive stance, considering each individual VOC, and study the source contribution to the O_3 formation.

Various analytical techniques have been documented in the existing literature to identify and trace the source of VOCs in the atmosphere. These analytical techniques encompass various methods, such as spectroscopy and inductively coupled plasma–mass spectrometry (ICP–MS) [28], laser-induced breakdown spectroscopy, portable modular biological mass spectrometry (MoBiMS) [29], proton transfer reaction–mass spectrometry (PTR–MS) [30, 31], and membrane inlet–mass spectrometry (MI–MS) [32]. While these traditional techniques are used for monitoring both atmospheric organic and inorganic volatile compounds, as well as volatile organohalogen compounds (VOHCs) in the gaseous phase [29, 33–37]. However, their scope of application is constrained due to inherent limitations such as poor quantification capacity, limited detection range, intricate and costly procedures, and the need for highly skilled personnel [29, 38]. Consequently, there exists a compelling demand for the development of a rapid and straightforward analytical method capable of furnishing a standardized and accurate approach to tracing VOCs sources in a given area of interest across all concentration levels in the atmospheric environment. This technique aims to overcome the above limitations observed in VOCs analysis,

improve the detection capability, and minimize the analysis time of VOCs. This provides an effective way of monitoring the air quality of the atmospheric environment.

In this study, we utilized a mobile laboratory navigation vehicle mounted with a portable self-developed device based on time-of-flight mass spectrometry (TOFMS) coupled with vacuum ultraviolet–single-photon ionization (VUV–SPI). This configuration facilitates real-time detection and monitoring of atmospheric pollution while concurrently tracing VOCs emission sources across the entire concentration range. In addition, we compile a comprehensive VOCs fingerprint library for distinct sources in Suzhou, Jiangsu Province, China. The ease of spectral interpretation is enhanced through the use of hyperspectral imaging, soft ionization sources, and the ability to ionize molecular ions, particularly for analytes in complex matrices [39]. TOFMS has been extensively utilized in the field of environmental air monitoring and inspection of industrial pollutions, as evidenced by its widespread application [40–42]. The method demonstrated excellent performance besides its good detection and quantification limits (LOD and LOQ) and a small range of relative standard deviation (RSD).

Methodology

Vehicle platform

The Puwei AQM-100 atmospheric navigation vehicle, modified by Suzhou Weimu Intelligent System Co., Ltd., utilizes an IVECO car from Navico, Ltd., Nanjing, China, for online atmospheric air monitoring. This platform is capable of capturing real-time concentration distributions of diverse VOCs. The system is equipped with various instruments to facilitate continuous monitoring operations for 24 h. These include an SPI–MS instrument (TMS-400) and a mass analyzer, a meteorological monitoring sensor (PSG04175 Leeds, LS12 2QQ, England), and an uninterrupted 6 kW high-power supply generator (DXGN6000, EM POWER, Florida US) are installed. Figure 1 illustrates the setup. Furthermore, a global positioning system (GPS receiver) (NV08C-CSM, Montlingen, Switzerland) to provide geographical data. The meteorological sensor is responsible for monitoring various meteorological parameters, including wind speed and direction, temperature, humidity levels, and atmospheric pressure. Real-time air pollution data are visualized on an electronic map through the utilization of the Air Scan System Software.

The vehicle comprised three distinct components: a front driver seat area similar to standard vehicles, a middle operating room that houses the GPS receiver for the purpose of monitoring geographical data, and a rear instrument compartment.

Experimental site

In this study, the geographical locations of the sampling sites are depicted in Fig. 2. The sites were located 100 km east of Shanghai and 200 km from Nanjing, with an average elevation ranging from 3.5 to 5 m above sea level. The sampling sites experience a subtropical monsoon climate characterized by four distinct seasons, similar to the climates of Shanghai, Hangzhou, and Nanjing cities [9]. To understand the spatial distribution and seasonal variations of VOCs concentration in Suzhou, Jiangsu Province, China (31° 18′ 14.69″ north latitude and 120° 35′ 43.37″ east longitude), the details of the sampling navigation routes are shown in Additional file 1: Fig. S1a, b. The monitoring experiment on atmospheric VOCs was conducted using an online mobile laboratory instrument during morning rush hours (8:00–9:00 a.m.) and in the evening (5:30–6:30 p.m.) from February 2022 to January

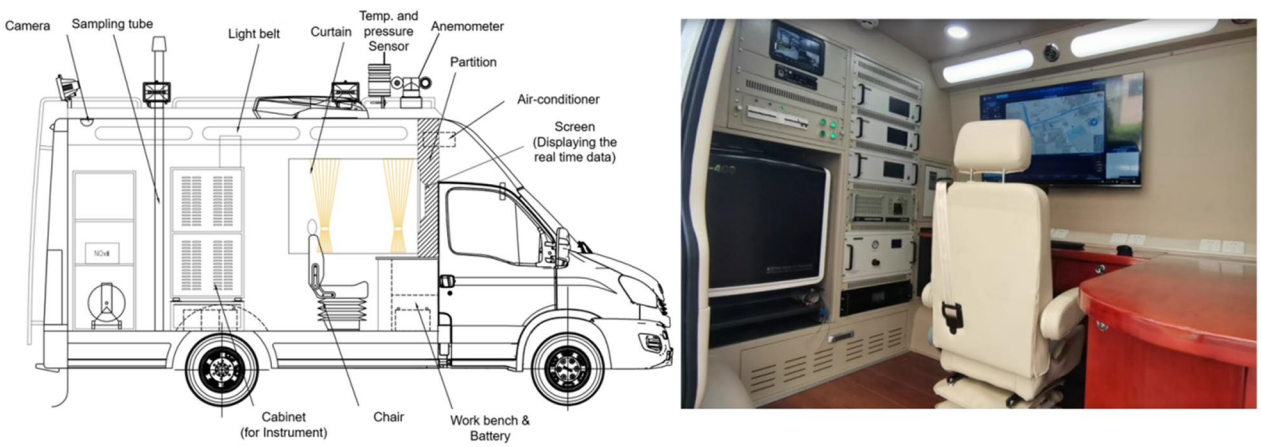

Fig. 1 Schematic diagram and photograph of the vehicle

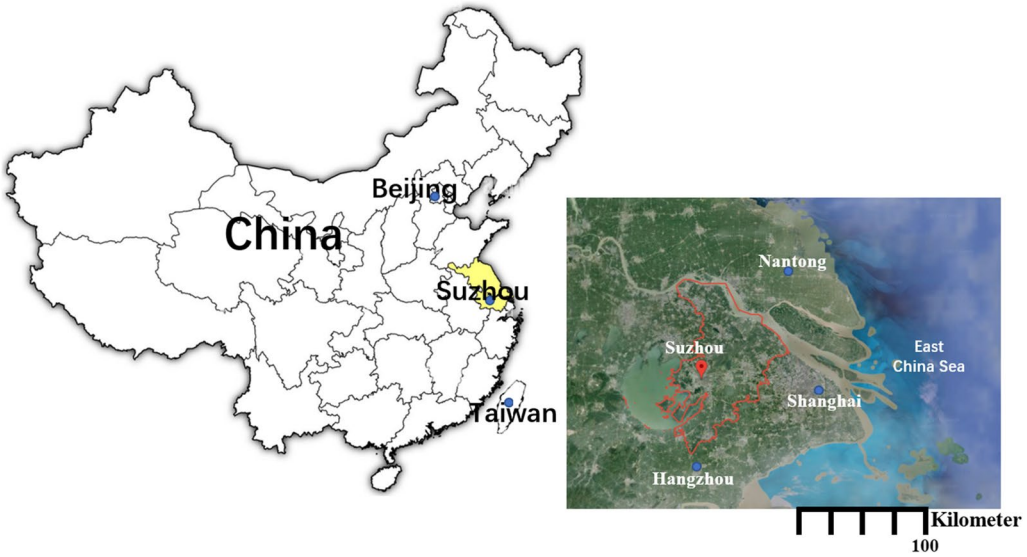

Fig. 2 Map of the study area: Suzhou China

2023 along the industrial park. In this study, the overall average atmospheric VOCs concentration was determined by calculating the average concentration for each sampling period under specific weather conditions. Six samples were collected each for winter (December to January), and summer (July to August), both during morning rush hours and in the evening. The average concentration was computed for each category as follows: the average concentration of VOCs for each of the four subgroups, namely, morning rush hours and evening during winter and summer. Subsequently, after obtaining these subgroup averages, the overall average concentrations during the monitoring period were determined.

SPI–TOFMS instrument

In the present study, a self-made integrated single-photon ionization–time-of-flight mass spectrometry (SPI–TOFMS) was employed to trace the source of VOCs. The system consists of several components, including a membrane inlet, an ionization system, a data acquisition system, a vacuum system, an electrical system, and a reflection TOFMS. The schematic diagram of the instrument is illustrated in Fig. 3. The dimensions of the SPI–TOFMS instrument are 50 cm × 50 cm × 50 cm, and it has an approximate weight of 50 kg. The device is equipped with a battery and a mechanical pump, allowing for its utilization in vehicles and mobile operations.

The pumping system comprises a scroll dry pump (SH110, Varian, Palo Alto, CA, USA) with a flow rate of 1 $Lmin^{-1}$ and a molecular turbo pump (V301, Varian, Palo Alto, CA, USA) with an operating speed of 300 Ls^{-1}. This ensures the requisite air pressure and optimal functionality. The dry pump operates at a pressure of approximately 200 Pa, which is supplied by the primary vacuum system. In addition, the molecular pump achieves a vacuum level that exceeds 2.1×10^{-3} Pa, thereby meeting the analytical specifications. The instrument demonstrates a rapid response speed in fractions of seconds and is capable of detecting 10 spectra per second. In addition, the SPI–TOFMS instrument is equipped with a high-speed data acquisition card, specifically the 1 GS/s Keysight U5309 (Keysight Technologies, USA), which enhances the efficiency of data processing and enables an extended collection period.

Membrane inlet system

The portable TOFMS is equipped with an inlet system consisting of a membrane inlet (MI) and a capillary inlet (CI). In the present study, the VOCs were gathered and underwent filtration using a silicon sheet membrane made of 90% polydimethylsiloxane (PDMS) from (Technical Production, Inc., St. Louis, MO, USA). The membrane had an effective diameter of 20 mm and a thickness of 50 μm. VOCs were introduced into the ionization region using a vacuum pump with a pumping speed of 1 $Lmin^{-1}$.

Single-photon ionization (SPI)

The SPI system comprises essential components, including a vacuum ultraviolet (VUV) lamp, an ionization chamber, a derivation electrode, a focus electrode, an output electrode, and a lens, as shown in Fig. 3. VUV lamps (low-pressure Krypton discharge lamps) are sourced from MgF_2 (Heraeus, Germany), are used to

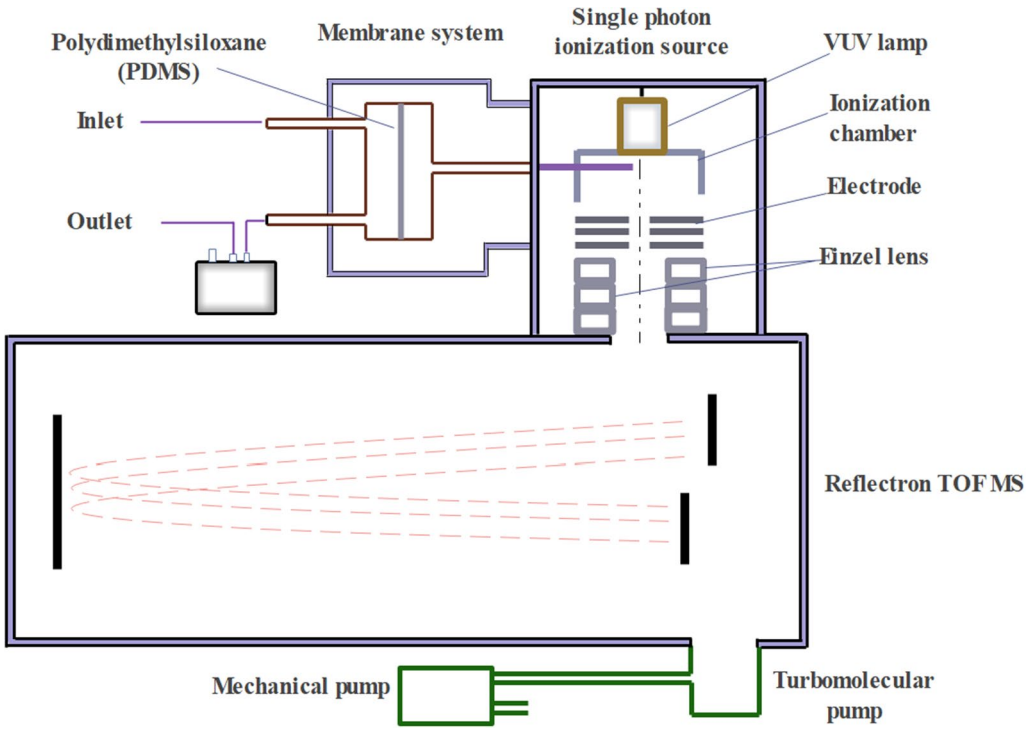

Fig. 3 Schematic diagram of the SPI–TOFMS-instrument

initiate the ionization process and generating photons at 10.6 eV. Notably, it is worth mentioning that only VOCs molecules possessing an ionization potential (IP) below 10.6 eV can be ionized into molecular ions without undergoing fragmentation. Gases like H_2, O_2, N_2, and Ar remain impervious to ionization. The focus electrode directs ionized molecules towards the mass analyzer. The transmission path is sealed and kept short to maintain high gas sample flow at 1000 $mLmin^{-1}$, allowing for more ionization to occur. When the VUV lamp is ignited with a voltage of 1100 V, the intensity of ions produced is directly proportional to the current flowing through the lamp and it can be regulated to a value of 1 mA. Lenses play a crucial role in the optimization of ion beam performance by facilitating the concentration of ions, thereby improving ion transmission efficiency, enhancing detection signal sensitivity, and mitigating the risk of mechanical misalignment.

Time-of-flight mass spectrometer (TOFMS)

The configuration of the SPI–TOFMS system consists of several distinct components, including a double-pulse acceleration region, a drift tube, a reflector, and an ion detector, as illustrated in Fig. 3. The development of TOFMS was initially based on an apparatus designed by Dodonov [43]. When ions with the same energy level but different mass-to-charge ratios traveling at a specific speed, they experience uniform acceleration in an electrostatic field with the measurement scan frequency of 10 kHz. This acceleration results in the ions having the same kinetic energy, and they subsequently reach the detector by passing through the drift tube. Lighter ions arrive earlier than the heavier ions, and their spectra are subsequently recorded. Determining the time of flight of each ion facilitates subsequent analysis. Peak integration and data acquisition were conducted using the Xcalibur® software (version 2.2 SP1.48; TFS, San Jose, CA, USA), which is embedded in the instrument system. The duration of each scan is approximately 100 ms, as determined by the experimental conditions, and can be adjusted to meet specific requirements.

Positive matrix factorization (PMF) model

Positive matrix factorization (PMF) is a robust multivariate factor analysis technique used to decompose a matrix of sample-specific data into two matrices: factor contributions and factor distribution. An analyst conducts an analysis of the matrices to ascertain the sources that are represented, using observations from receptor sites [44]. In this study, Eq. 1 depicts the concentration of the *j*th chemical species in the *i*th samples, which is influenced by *p* independent sources:

$$x_{ij} = \sum_{k=1}^{p} g_{ik} f_{kj} + e_{ij} \quad (1)$$

where x_{ij} is the jth species concentration measured data matrix in the ith sample variable, g_{ik} is the species contribution of the kth source to the ith sample, f_{ki} is the jth species fraction from the kth source, e_{ij} is the residual for each species, and p is the total number of independent sources. where $i=1,\ldots, m$ species, $j=1,\ldots, n$ samples, $k=1,\ldots, p$ sources.

In relation to the input for the PMF model, it is not necessary to utilize all of the collected data. This is because the PMF model operates under the fundamental assumption of non-reactivity and mass conservation [45]. Without prior knowledge of the sources of VOCs, the technique generates source profiles and time series matrices that depict the contribution of each source to the overall VOCs emissions. In the PMF, it is a requirement that the sources possess species values that are non-negative. In addition, it is not permissible for any sample to have a negative contribution originating from a source.

To solve the PMF equation, enabling the examination of the distribution for each species and evaluation of the solution, stability, an objective function can be minimized by considering the inherent uncertainties associated with each observation, as indicated in the following equation:

$$Q = \sum_{i=1}^{m} \sum_{j=1}^{n} \left[e_{ij} / s_{ij} \right]^2 \quad (2)$$

where *sij* represents the uncertainty estimate of a data point corresponding to the jth species measured in the ith sample. The analysis was conducted using software version 5.0, and Eqs. 3 and 4 were utilized to compute the uncertainties associated with the input data sets. When the concentration of VOCs falls below the MDL, Eq. 3 is applied; conversely, Eq. 4 is utilized for VOCs concentrations that exceed the MDL. However, in cases where values fell below the detection limit, they were replaced with half of the detection limit. The overall uncertainty for these substituted values was determined to be 5/6 of the detection limit, as indicated in the following equation:

$$\text{Unc} = \frac{5}{6} x \text{MDL} \quad (3)$$

$$\text{Unc} = \sqrt{(\text{Error fraction} \times \text{Conc.})^2 + (0.5 \times \text{MDL})^2} \quad (4)$$

where MDL represents the detection limit, and the error fraction can be adjusted within the range of 5–20% depending on the concentration level [46]. In this study, the Error fraction was determined through empirical means, specifically set at 10% [47], based on their previous experience.

The selection of appropriate species for the PMF analysis was determined by considering the following: (1) the selected VOCs species have the highest photochemical reactivity; (2) they serve as the fundamental tracer for the target industrial byproduct around the study area; (3) they were detected in significant amounts; and (4) highly reactive species with rapid atmospheric reactivity were also omitted. Finally, species that serve as effective indicators for identifying pollution sources were appropriately selected and used for the analysis.

Results and discussion

Performance verification of SPI–TOFMS

The integrated SPI–TOFMS instrument was characterized using a standard mixture comprising typical 48 VOCs from the Photochemical Assessment Monitoring Station (PAMS-48), as presented in Additional file 1: Table S1. Figure 4 illustrates the linearity and sensitivity parameters of benzene standard solutions within a concentration range of 1, 5, 10, 20, and 50 ppbv. The performance curves demonstrated a high level of linearity, with an R^2 value of 0.99. This indicates that the SPI–TOFMS technique demonstrates excellent sensitivity and repeatability for VOCs detection. The determination of the MDL and MQL was conducted through the measurement of the signal-to-noise ratio. MDL was defined as an S/N ratio of 3, while MQL was determined with an S/N ratio of 10. The MDL and MQL were determined to be 0.090 ppbv and 0.300 ppbv, respectively. The MDL presents the remarkable sensitivity of the technique, with a relative standard deviation (RSD, $n=4$) of 4%. Moreover, the mass resolution surpassed a value of 1500. This suggest that the SPI–TOFMS instrument demonstrates analytical reliability and stability when used for the detection and

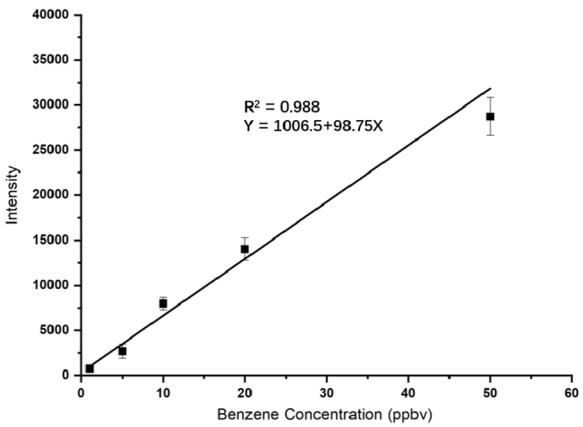

Fig. 4 Calibration curve of benzene from 1, 5, 10, 20, and 50 ppbv

Table 1 Measured concentrations selected for PMF model simulation

VOCs species	Concentrations (ppbv)	MIR[a]	O_3 formation (ppbv)[b]
Ethane	12.81	0.321	4.112
n-Butane	3.57	1.33	4.748
Methylchloride	2.4	0.042	0.101
Xylene	3.33	7.17	23.876
Propane	3.2	0.56	1.792
n-Pentane	4.05	1.56	6.318
i-Pentane	6.01	1.65	9.916
Benzene	2.99	0.78	2.332
Hexane	3.88	1.55	6.014
Toluene	2.75	4.02	11.055
Trimethylbenzene	0.37	32.7	12.099
n-Octane	3.82	1.15	4.393
Styrene	6.08	1.7	10.336
n-Heptane	2.31	1.37	3.164
Ethene	6.3	8.64	54.432

[a] MIR denotes maximum incremental reactivity, and updated MIR values are obtained from [68]

[b] [VOC] × MIR, ppbv

monitoring of VOCs and other atmospheric pollutants in complex atmospheric environments, offering acceptable precision and exhibiting a high level of sensitivity.

Analysis of the navigation monitoring data

The VOCs commonly found in the atmospheric environment were identified and listed in Table 1 and Additional file 1: Table S2. A total of 41 VOCs constitute 99.8% of the total mass of the detected VOCs species during multiple series of navigation monitoring experiments conducted throughout the experimental period. These VOCs serves as a typical tracer for different sources of environmental emissions. The VOCs that are commonly found include n-pentane, styrene, hexane, and toluene. Alkanes and aromatics constituted the primary VOCs species that were assessed during the field detection experiments conducted for monitoring purposes.

Source profile identification and PMF analysis

In the present study, the PMF technique was employed to analyze the measured VOCs at various monitoring sites, leading to the identification of seven distinct factors. These factors profiles are presented in Fig. 5 and Additional file 1: Table S3. The major group of VOCs detected

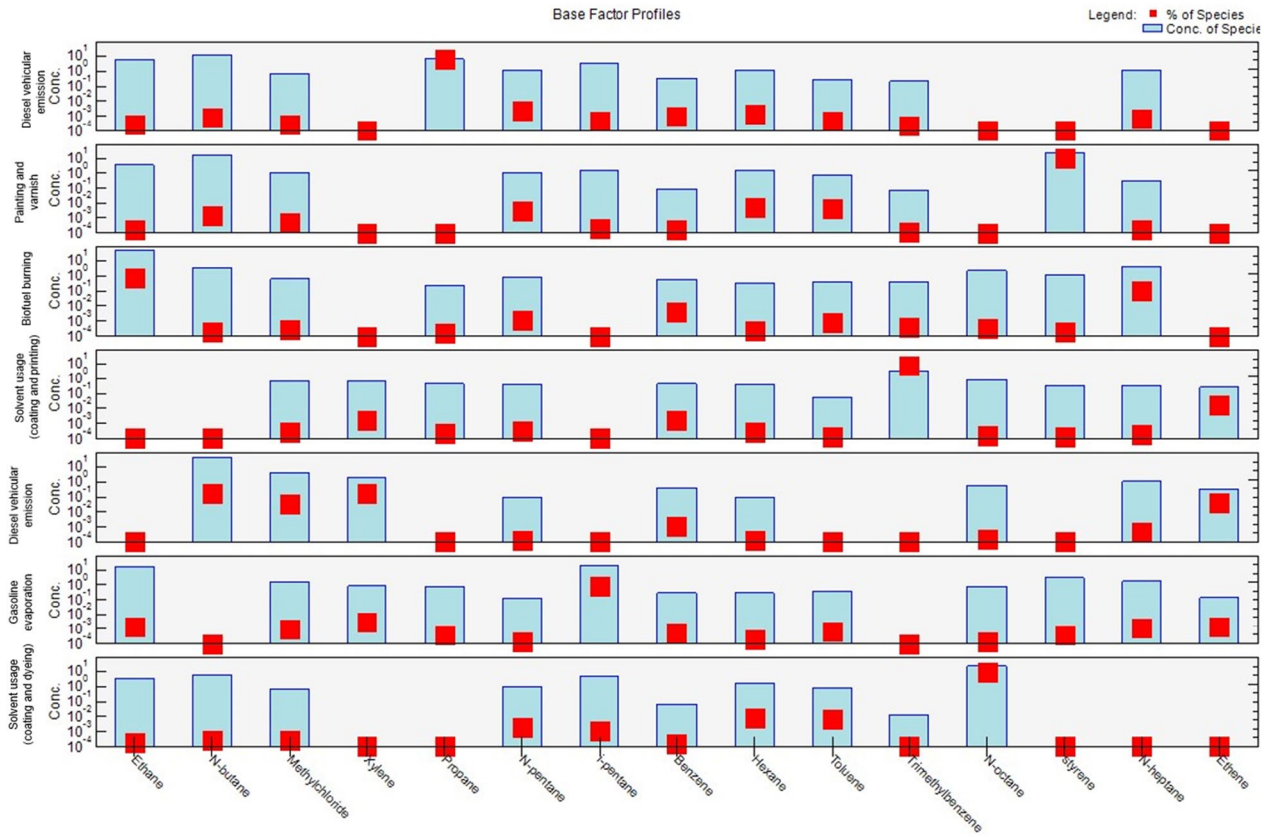

Fig. 5 Factor profiles derived from the PMF models used to predict the VOCs sources in the Suzhou industrial park

during the monitoring experiment were alkane, aromatics, and alkenes. Alkanes were found to be the most prevalent group of compounds detected, with their primary sources being vehicle exhaust and industrial processes. This makes them a significant source of VOCs in urban atmospheres [48, 49].

Factor 1 reveals a high abundance of n-butane, ethane, propane, and *i*/*n*-pentane, along with smaller amounts of heptane, hexane, and methyl chloride. n-butane and ethane were identified as dominant VOCs species, collectively constituting 60% of the overall VOCs within the source profile. Ethane, propane, and butane are natural gases [50], constituting 20% of the total VOCs detected in this source profile. These serve as tracers for vehicle emissions, specifically those originating from diesel combustion engines. Based on the PMF analysis, Factor 1 has been identified as diesel vehicular emissions. In Factor 2, the presence of styrene accounts for 70% of the total identified VOCs species in the profile. In addition, a significant amount of butane and ethane compounds were also identified in the profile. Styrene and butane, has been identified as fundamental tracers for industrial solvents, as stated by Gabriel [51]. Furthermore, Borbon et al. [52] assert that styrene, butane, and ethane are frequently employed as solvents in the painting, printing, and textile industries. Hence, Factor 2 is associated with paint and varnish, primarily for coating and ink applications in the rubber painting, printing, and textile industries in Suzhou [53, 54]. Factor 3 profile suggests ethane as the highest contributor to the VOCs accumulation, constituting approximately 80% of the total VOCs. In addition, compounds such as butane, heptane, and octane were identified in this profile, collectively accounting for 15% of the total VOCs species present. For a more precise elucidation of this source, it should be noted that these VOCs are primarily emitted from biomass burning, specifically biofuel, as well as certain vehicular emissions, such as those from diesel combustion engines. Vehicular emissions are linked to a certain proportion of other VOCs species, such as pentane, benzene, trimethylbenzene, and xylene, which were not detected in this particular factor. Furthermore, the significant presence of ethane suggests that Factor 3 has been identified as biomass/biofuel burning [55].

Factor 4 is predominantly characterized by the presence of trimethylbenzene, which constitutes 65% of the total VOCs species in this source profile. In addition, significant amounts of xylene, benzene, and styrene are also detected. These compounds are frequently released as by-products of industrial processes that involve the use of organic solvents, such as painting, printing, and coating [52]. With regard to factor 5, the highest proportions of butane, ethene, methyl chloride, and xylene were observed. These species have a close association with vehicular emissions, particularly those resulting from diesel engine combustion. This process releases significant amounts of butane, ethane, and xylene [56]. Thus, Factor 5 was refer to as a diesel engine vehicular emission. Factor 6 is characterized by a significant presence of lower alkanes, such as ethane, pentane, and heptane, along with notable concentrations of benzene, styrene, and xylene. The presence of a significant proportion of lower alkanes and some certain aromatic compounds has been identified as the reliable tracer of emissions from vehicles powered by gasoline [57]. Therefore, Factor 6 is associated with gasoline evaporation. The seventh factor profile, which is factor 7, is predominantly influenced by a significant quantity of octane. Octane is frequently utilized as a solvent in various industries such as paint, adhesives, and liquid process photocopiers [57].

VOCs source contribution and fingerprint in Suzhou compare with other cities

Over the past three decades, Suzhou has undergone rapid economic growth, urbanization, and industrialization, resulting in a marked escalation in vehicular traffic. According to the PMF analysis results, the primary emission sources contributing to the total VOCs and predominant anthropogenic activities in the city are vehicular emissions; industrial activities such as coating, painting, and printing; and biofuel burning. These sources are similar to those observed in Nanjing city [58]. Figure 6 shows the percentage contribution of the source profile of anthropogenic VOCs in the city. Li et al. [59] conducted a comparison of total VOCs emissions and their concentration levels in Suzhou with those of major cities in China, such as Beijing, Tianjin, and Shanghai. As an industrial hub of Jiangsu Province, Suzhou has the most concentrated industrial enterprises and the densest population with the highest car population, making it the only city in Jiangsu Province with a population of more than 12 million [60]. Among the various sources of atmospheric VOCs in the city, vehicular emissions play a significant role. Specifically, vehicular diesel emissions contribute to 27% of total VOCs emissions, while gasoline evaporation accounts for 15% of the total VOCs emissions. Considering gasoline evaporation and diesel vehicular emissions as part of vehicular emissions, this is marked as the primary source of atmospheric VOCs in the city, comprising over 40% of the total ambient VOCs detected by the SPI–TOFMS and categorized using the PMF model. Industrial processes and solvent usage involve the use of organic solvents by industries and daily life activities (including coating, painting, and printing, while daily life activities encompass building, decoration, and cleaning) in daily production and manufacturing processes, leading

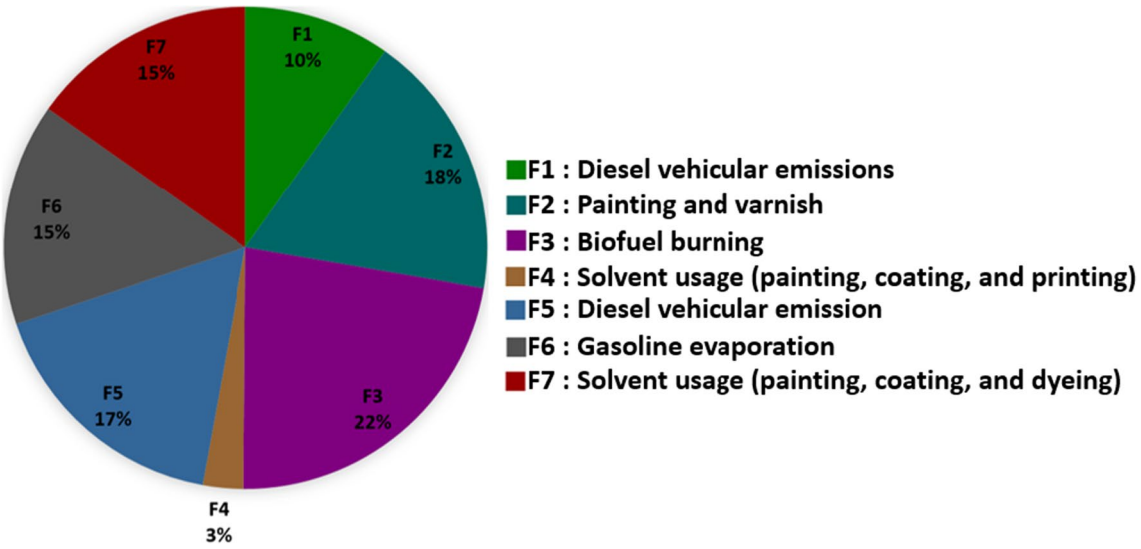

Fig. 6 Source contributions to ambient VOCs in Suzhou

to the large-scale production of various varieties of VOCs into the atmosphere. During our navigation experiment, SPI–TOFMS was able to detect various VOCs related to dyeing, printing, coating, and painting industries (including styrene, butane, ethane, trimethylbenzene, xylene, and benzene). These VOCs are responsible for 36% of the total VOCs detected by the instrument, thereby establishing them as the second most significant source as determined by the model. Biofuel burning was identified as the third major source of VOCs emissions in the city, following vehicular emissions and industrial solvents. contributing 22% to the total detected ambient VOCs. Therefore, vehicular emissions can be considered a significant contributor to VOCs in the city.

In general, the concentration of VOCs follows the order of roadside, industrial sites, and residential areas, which can be attributed to the increasing number of vehicles in Suzhou [61]. Several studies conducted in various Chinese cities consistently show that motor vehicles are the main contributors to ambient VOCs [62, 63]. For instance, research conducted in Shanghai has confirmed that motor vehicles play a substantial role in VOCs emissions [63]. Considering the predominant industrial activities in Suzhou, which encompass painting, coating, dyeing, and textile production, it can be deduced that the principal emissions arising from these sectors are organic solvents employed in their routine operations.

VOCs profiling in wastewater treatment

VOCs are the primary constituents of the odor emitted from wastewater and sewage sludge composting plants, and they are generally associated with odorous nuisances and health risks. In our navigation experiment around the wastewater treatment plant, we selected four major treatment units of the composting plant as monitoring locations, namely, the dewatered unit, dewatered sludge, fermentation workshop, and product units. The product units exhibited the highest concentration of VOCs emissions at 13.367 ppbv, followed by the fermentation workshop and dewatered sludge, with emissions of 9.290 ppbv and 3.240 ppbv, respectively, as presented in Table S4 in the supporting information. The detected VOCs families included halogenated hydrocarbons, aldehydes, and aromatic compounds. Halogenated hydrocarbons, particularly bromodichloromethane, were the most abundant compounds in all samples detected by SPI–TOFMS in this area. The product units differed from the other sampling units, as their typical compounds were toluene, benzene, and styrene, all of which were the products of the latter stages of composting. Among the treatment units, the fermentation workshop units had the highest halogenated hydrocarbon (bromodichloromethane) concentration. Acrolein, bromodichloromethane, and benzene were the major contributors, contributing to the increased atmospheric VOCs and ozone formation potential in the surrounding air.

VOCs tag identification library

Pollution leakage accidents can occur abruptly. To enhance the efficacy of pollution control techniques, it is imperative to promptly identify the distinct characteristics of VOCs that contribute to pollution and trace their emission sources. Therefore, it is imperative to establish a comprehensive database library that includes

a representative VOCs tracer for each emission source. This library will serve as a valuable resource for efficiently tracking different sources of emissions during the control process.

Additional file 1: Table S5 provides a comprehensive comparison between our navigation experimental SPI–TOFMS and traditional techniques, specifically GC–MS, portable GC–FID, and GC–MS. The comparison spans various critical aspects, including the detection of specific VOCs, sorbent phase, qualitative/quantitative mode, sample types, and overall performance. Our navigation experimental setup, enabled by SPI–TOFMS, facilitates real-time and on-site monitoring, capturing the dynamic nature of VOC emissions in diverse environmental settings. This stands in contrast to traditional techniques that may provide delayed or less flexible measurements.

Table 2 displays VOCs tracers used to identify different sources. Acrolein, bromodichloromethane, and benzene serve as tracers for sewage treatment, while toluene and heptane are utilized as tracers for printing and dyeing. Butane, octane, and xylene are employed as tracers for oil-spraying plants. These results are consistent with previous studies, which have shown that toluene is the predominant pollutant from the printing and dyeing industries [52–54]. Similar to the findings of Ravina et al. [64], it was observed that benzene and bromodichloromethane serve as the primary pollutants in sewage treatment plants. These findings demonstrate the stability and reliability of our instrument for emergency monitoring.

According to the real-time navigation monitoring results of SPI–TOFMS in Suzhou, a wide range of VOCs were detected. Furthermore, several emission sources, including wastewater and sewage sludge, printing and dyeing plants, and oil spraying plants, were identified and analyzed using VOCs tracers associated with these sources. Attributes characterizing the VOCs species are shown in Table 2. SPI–TOFMS is a promising technique for real-time detection at gas leakage accident sites, providing an accurate reference for emergency detection and monitoring VOCs emission sources.

Table 2 Emissions source and measured VOC at the navigation monitoring experiment site in Suzhou

VOCs species	Sewage treatment plants (ppbv)	Printing and dyeing plants (ppbv)	Oil spraying plant (ppbv)
n-Butane	0.63	0.89	**6.20**
Xylene	0.58	0.76	**5.21**
Acrolein	**8.08**	0.48	0.70
Bromodichloromethane	**3.0**	–	0.12
Benzene	**4.67**	0.122	0.72
Toluene	0.93	**9.41**	1.33
n-Octane	0.41	0.49	**2.87**
n-Heptane	0.86	**2.47**	–

Bold values signify the presence of higher concentration compared with others or signify the major tracer

Ozone formation potential (OFP)

The ozone formation potential (OFP) serves as a significant index for quantifying and elucidating the role and contribution of individual VOCs in the formation of ozone in the atmosphere. Theoretically, controlling the NO_x emission and VOCs in the atmosphere will lead to a reduction in atmospheric ozone. The relationship between ozone formation and precursor concentration is not solely characterized by a linear correlation. The quantity of ozone in NO_x conditions is contingent upon the level of radicals produced from the reaction of VOCs. According to Carter et al. [65], the formation of ozone is limited at lower NO_x concentrations lower. Previous studies have proposed various approaches to investigating the role of specific VOCs in the photochemical process [66, 67]. In this study, the concept of maximum incremental reactivity (MIR) is used to evaluate the ozone formation potential of the individual VOCs. The techniques and process employed to establish the MIR scale, as outlined in this study, are thoroughly described by Carter et al. [68], and references therein, and those reports should be consulted for details. Briefly, the reactivity scale is determined by calculating the relative ozone impacts, expressed as mass of additional ozone formed per mass of VOCs added to the emissions, for various compounds under various atmospheric conditions, given a chemical mechanism for the compounds and other relevant atmospheric species, models for various atmospheric conditions, and a modeling and reactivity assessment procedure. Incremental reactivity can be conceptualized as the result of two underlying factors: (1) kinetic reactivity, which refers to the proportion of emitted VOCs that undergo chemical reactions in the specific pollution scenario under consideration and (2) mechanistic reactivity, which quantifies the amount of ozone formed in relation to the amount of VOCs that have reacted. The significance of this concept is that this provides a means to factor out to a certain extent, the impact of a VOC's reaction rate from all the other mechanistic aspects which affect reactivity. Since the only aspect of the VOC's mechanism which affects kinetic reactivities is the VOC's rate constants, which generally are known, the ability of a mechanism to predict kinetic reactivities are not considered to be particularly uncertain. MIR computes the OFP of individual VOCs by considering its reactivity mechanism, taking into account the impact of the different reaction mechanisms and VOCs and NO_x

ratio, on the formation of ozone [24]. The ozone formation is determined by the multiplication of the concentration of each VOCs species by its corresponding MIR coefficient as expressed by the equation:

$$\mathrm{OFP} = \mathrm{VOCs}_{(i)} \times \mathrm{MIR}_{(i)}$$

where VOCs *(i)* represents the concentration of individual VOCs, and MIR *(i)* denotes the maximum incremental reactivity of VOCs species *i*.

The results presented in Table 1 highlight the primary factors that contribute to ozone formation in Suzhou. Ethane, trimethylbenzene, xylene, toluene, and styrene have been identified as the predominant substances contributing to the formation of ozone in the city, collectively contribute for 67% of the total ozone production. Despite alkanes having the highest volume fraction among the total identified VOCs, their photochemical reactivity is comparatively low, leading to a diminished impact on ozone formation. On the contrary, aroma compounds, despite their lower percentage contribution to the total VOCs in comparison with alkanes, play a more significant to the formation of ozone in Suzhou.

Dynamics analysis of NO_x and O_3 in Suzhou

The average concentration of NO_x fluctuated between 6.540 and 21.100 ppbv during winter and 3.950 to 16.870 ppbv during summer, respectively. The trends of NO_x concentrations in Suzhou were similar to those in Shanghai [69]. As illustrated in Fig. 7, the daily average concentration of NO_x in Suzhou exhibited a bimodal distribution: the first peak appeared between 08:15 and 08:45 a.m. in the morning, and the second peak occurred between 5:45 and 6:15 p.m. in the evening. Interestingly, the concentration of the second peak was significantly lower than the morning peak, possibly linked to higher emissions from diesel vehicles [70]. High concentrations were observed during the winter morning rush hours, while lower concentrations were recorded during summer nights. The seasonal patterns of NO_x in our study align with those reported in other studies [71, 72]. In general, NO_x concentrations were higher in winter, and the change in the concentration trend was associated with meteorological conditions. The analysis suggests that NO_x concentrations in the city are lower during summer than the winter period due to temperature inversions. In contrast, O_3 concentrations are higher during summer than winter due to longer days and higher solar radiation, leading to a higher rate of photochemical reaction. In addition, during summer, the reduction of NO_x leads to an enhancement in OH radicals, resulting in higher O_3 production. This enhancement of summer O_3 is offset by a decrease in VOCs.

Conclusion

The emissions sources of volatile organic compounds (VOCs) were traced and identified in China's city Suzhou. The analysis of their contribution to ozone formation was conducted using a single-photon ionization–time-of-flight mass spectrometer (SPI–TOFMS). The study utilized the positive matrix factorization

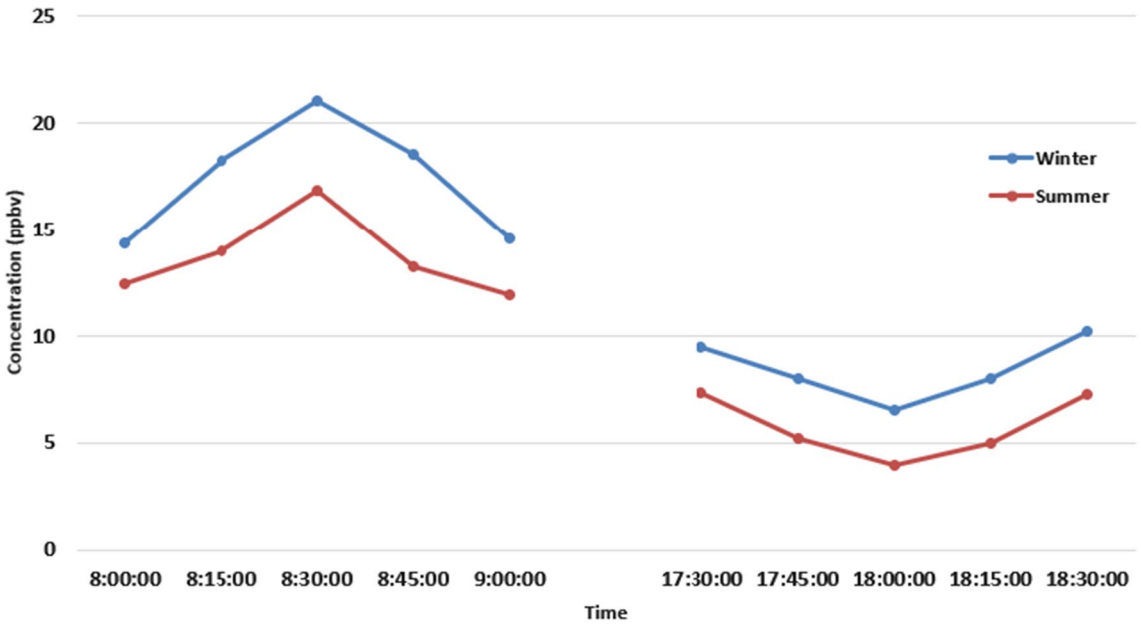

Fig. 7 Daily average concentration of nitrogen oxide (NO_x) in Suzhou

(PMF) model to conduct an analysis of the apportionment of VOCs sources. The results of the analysis identified three main sources of VOCs emissions: vehicular emissions (F1, F5, and F6), industrial solvents (F2, F4, and F7), and biofuel burning (F3). Alkanes were the most prevalent VOCs species, constituting 60% of the overall VOCs. Aromatic hydrocarbons and alkenes were also present, albeit in lower quantities. Aromatics and alkenes were observed to make a substantial contribution to ozone formation, as evidenced by the results of the maximum incremental reactivity coefficient (MIR). The study suggests that efficient control of ozone formation in Suzhou can be achieved by reducing emissions of ethene, trimethylbenzene, xylene, styrene, and toluene originating from solvent-based industries, vehicles, and biofuel combustion. The primary contributors to the potential for ozone formation in Suzhou were identified as sources related to transportation and industrial solvents. In addition, the utilization of SPI–TOFMS facilitated the development of an identification library for emergency monitoring in the event of pollution accidents, thereby enabling the precise localization of emission sources. The study proposes that the use of SPI–TOFMS enables the rapid and direct monitoring and tracing of VOCs emission sources in the atmospheric environment. This method shows promise for efficiently inspecting and controlling air pollution. Furthermore, the development of targeted pollution control strategies requires collaboration between researchers, policymakers, and industries. Implementing effective emission reduction measures, promoting sustainable practices, and adopting cleaner technologies are pivotal in mitigating ozone pollution.

Abbreviations

CI	Capillary inlet
ICP	Inductively coupled plasma
IP	Ionization potential
LOD	Limits of detection
LOQ	Limits of quantification
MI	Membrane inlet
MIMS	Membrane inlet mass spectrometry
MIR	Maximum incremental reactivity
MoBiMS	Modular biological mass spectrometry
MDL	Method detection limit
MQL	Method quantification limit
MS	Mass spectrometer
OBM	Observation-based model
OFP	Ozone formation potential
O_3	Ozone
PDMS	Polydimethylsiloxane
PMF	Positive matrix factorization
PTRMS	Proton transfer reaction mass spectrometry
RSD	Relative standard deviation
SPI	Single-photon ionization
TOF	Time-of-flight
VOC(s)	Volatile organic compounds
VOHC(s)	Volatile organohalogen compounds
VUV–SPI	Vacuum ultraviolet–single-photon ionization

Supplementary Information

The online version contains supplementary material available at https://doi.org/10.1186/s12302-024-00872-2.

Additional file 1: Table S1. Linearity and sensitivity parameters of standard mixture of Photochemical Assessment Monitoring Station (PAMS-48). **Table S2.** Concentration Profiles of VOCs Emissions in Suzhou city. **Table S3.** Concentration Profiles of VOCs of the Seven Factors. **Table S4.** Concentration Profiles of VOCs Emissions in wastewater Treatment Units. **Table S5.** Comparison with other studies. **Fig. S1.** a. The vehicle experiment route in Suzhou industrial park. b. The vehicle experiment route in Suzhou wastewater treatment plant.

Acknowledgements

The authors sincerely appreciate the help of the analysts from Suzhou Weimu Intelligent System Co., Ltd, College of Information Science & Electronic Engineering, Zhejiang University, and Suzhou Mass Spectrometer Weixing Intelligent Technology Co., Ltd.

Author contributions

NSS and CQ: conceptualization, methodology, investigation, data curation, software, validation, writing—original draft and editing. FC and AMI: conceptualization, investigation, and review. XW, BBI, and GZ: supervision and editing. SAAA and MGI: data analysis, and figure drawing. GZ, XW, NSS, and CQ: investigation, writing—reviewing and editing. XW, CQ and GZ: supervision, resources, writing—reviewing and editing, project administration, and funding acquisition. All authors read and approved the manuscript.

Funding

This work was supported by the National Natural Science Foundation of China with grant nos. 62174147, 21927810, Key Research and Development Project of Zhejiang with grant nos. 2022C01141, and Dr. Li Dak Sum & Yip Yio Chin Development Fund for Regenerative Medicine, Zhejiang University.

Availability of data and materials

Not applicable.

Declarations

Ethics approval and consent to participate

Not applicable.

Consent for publication

Not applicable.

Competing interests

The authors declare no competing interests.

Author details

[1]Zhejiang University College of Information Science and Electronic Engineering, Hangzhou 310027, Zhejiang Province, China. [2]China National Environmental Monitoring Centre, Beijing 100012, China. [3]College of Biosystems Engineering and Food Science, Zhejiang University, Hangzhou 310058, China. [4]Zhejiang Zhoushan Hospital, Zhoushan 316021, China. [5]Department of Electrical Engineering, Aliko Dangote University of Science and Technology, Wudil 713101, Kano State, Nigeria. [6]Shanghai University School of Environmental and Chemical Engineering, Shanghai 200444, China.

Received: 11 November 2023 Accepted: 19 February 2024
Published online: 04 March 2024

References

1. Gariazzo C, Pelliccioni A, Di Filippo P et al (2005) Monitoring and analysis of volatile organic compounds around an oil refinery. Water Air Soil Pollut 167:17–38. https://doi.org/10.1007/s11270-005-8203-x
2. Petry T, Vitale D, Joachim FJ et al (2014) Human health risk evaluation of selected VOC, SVOC and particulate emissions from scented candles. Regul Toxicol Pharmacol 69:55–70. https://doi.org/10.1016/j.yrtph.2014.02.010
3. Shuai J, Kim S, Ryu H et al (2018) Health risk assessment of volatile organic compounds exposure near Daegu dyeing industrial complex in South Korea. BMC Public Health 18:1–13. https://doi.org/10.1186/s12889-018-5454-1
4. Sheng J, Zhao D, Ding D et al (2018) Characterizing the level, photochemical reactivity, emission, and source contribution of the volatile organic compounds based on PTR-TOF-MS during winter haze period in Beijing, China. Atmos Res 212:54–63. https://doi.org/10.1016/j.atmosres.2018.05.005
5. Agbroko SO, Covington J (2018) A novel, low-cost, portable PID sensor for the detection of volatile organic compounds. Sensors Actuators B Chem 275:10–15. https://doi.org/10.1016/J.SNB.2018.07.173
6. Beauchamp J, Wisthaler A, Grabmer W et al (2004) Short-term measurements of CO, NO, NO2, organic compounds and PM10 at a motorway location in an Austrian valley. Atmos Environ 38:2511–2522. https://doi.org/10.1016/J.ATMOSENV.2004.01.032
7. Su YC, Chen WH, Fan CL et al (2019) Source apportionment of volatile organic compounds (VOCs) by positive matrix factorization (PMF) supported by model simulation and source markers—using petrochemical emissions as a showcase. Environ Pollut 254:112848. https://doi.org/10.1016/j.envpol.2019.07.016
8. Wang XF, Li ML, Fang QQ et al (2021) Flexible electrical stimulation device with Chitosan-Vaseline®dressing accelerates wound healing in diabetes. Bioact Mater. https://doi.org/10.1016/j.bioactmat.2020.08.003
9. Zheng S, Xu X, Zhang Y et al (2019) Characteristics and sources of VOCs in urban and suburban environments in Shanghai, China, during the 2016 G20 summit. Atmos Pollut Res 10:1766–1779. https://doi.org/10.1016/j.apr.2019.07.008
10. Delfino RJ, Sioutas C, Malik S (2005) Potential role of ultrafine particles in associations between airborne particle mass and cardiovascular health. Environ Health Perspect 113:934–946. https://doi.org/10.1289/ehp.7938
11. Rumchev K, Spickett J, Bulsara M et al (2004) Association of domestic exposure to volatile organic compounds with asthma in young children. Thorax 59:746–751. https://doi.org/10.1136/thx.2003.013680
12. Sram RJ, Binkova B, Dostal M et al (2013) Health impact of air pollution to children. Int J Hyg Environ Health 216:533–540. https://doi.org/10.1016/j.ijheh.2012.12.001
13. Englert N (2004) Fine particles and human health—a review of epidemiological studies. Toxicol Lett 149:235–242. https://doi.org/10.1016/j.toxlet.2003.12.035
14. Dockery DW, Stone PH (2007) Cardiovascular risks from fine particulate air pollution. N Engl J Med 356:511–513. https://doi.org/10.1056/nejme068274
15. Pope CA, Burnett RT, Thurston GD et al (2004) Cardiovascular mortality and long-term exposure to particulate air pollution: epidemiological evidence of general pathophysiological pathways of disease. Circulation 109:71–77. https://doi.org/10.1161/01.CIR.0000108927.80044.7F
16. Sani SN, Zhou W, Ismail BB et al (2023) LC-MS/MS based volatile organic compound biomarkers analysis for early detection of lung cancer. Cancers (Basel) 15:1186. https://doi.org/10.3390/cancers15041186
17. Diab J, Streibel T, Cavalli F et al (2015) Hyphenation of a EC / OC thermal-optical carbon analyzer to photo-ionization time-of-flight mass spectrometry: an off-line aerosol mass spectrometric approach for characterization of primary and secondary particulate matter. Atmos Meas Tech 8:3337–3353. https://doi.org/10.5194/amt-8-3337-2015
18. Chang CC, Chen TY, Lin CY et al (2005) Effects of reactive hydrocarbons on ozone formation in southern Taiwan. Atmos Environ 39:2867–2878. https://doi.org/10.1016/j.atmosenv.2004.12.042
19. So KL, Wang T (2004) C3–C12 non-methane hydrocarbons in subtropical Hong Kong: spatial-temporal variations, source-receptor relationships and photochemical reactivity. Sci Total Environ 328:161–174. https://doi.org/10.1016/j.scitotenv.2004.01.029
20. Zhang X, Gao S, Fu Q et al (2020) Impact of VOCs emission from iron and steel industry on regional O3 and PM2.5 pollutions. Environ Sci Pollut Res 27:28853–28866. https://doi.org/10.1007/s11356-020-09218-w
21. Ling ZH, Guo H, Cheng HR, Yu YF (2011) Sources of ambient volatile organic compounds and their contributions to photochemical ozone formation at a site in the Pearl River Delta, southern China. Environ Pollut 159:2310–2319. https://doi.org/10.1016/j.envpol.2011.05.001
22. Ling ZH, Guo H (2014) Contribution of VOC sources to photochemical ozone formation and its control policy implication in Hong Kong. Environ Sci Policy 38:180–191. https://doi.org/10.1016/j.envsci.2013.12.004
23. Cheng H, Guo H, Wang X et al (2010) On the relationship between ozone and its precursors in the Pearl River Delta: application of an observation-based model (OBM). Environ Sci Pollut Res 17:547–560. https://doi.org/10.1007/s11356-009-0247-9
24. Cardelino CA, Chameides WL (1995) An observation-based model for analyzing ozone precursor relationships in the urban atmosphere. J Air Waste Manag Assoc 45:161–180. https://doi.org/10.1080/10473289.1995.10467356
25. Zhang YH, Su H, Zhong LJ et al (2008) Regional ozone pollution and observation-based approach for analyzing ozone-precursor relationship during the PRIDE-PRD2004 campaign. Atmos Environ 42:6203–6218. https://doi.org/10.1016/j.atmosenv.2008.05.002
26. Russell A, Dennis R (2000) NARSTO critical review of photochemical models and modeling. Atmos Environ 34:2283–2324. https://doi.org/10.1016/S1352-2310(99)00468-9
27. Ling ZH (2011) SOURCE~1.PDF. 2310–2319.
28. Shaltout AA, Boman J, Welz B et al (2014) Method development for the determination of Cd, Cu, Ni and Pb in PM2.5 particles sampled in industrial and urban areas of Greater Cairo, Egypt, using high-resolution continuum source graphite furnace atomic absorption spectrometry. Microchem J 113:4–9. https://doi.org/10.1016/j.microc.2013.10.009
29. Alcalde-Vázquez R, Moreno-Pedraza A, Rosas-Román I et al (2022) MoBiMS: a modular miniature mass analyzer for the real-time monitoring of gases and volatile compounds in biological systems. Microchem J. https://doi.org/10.1016/j.microc.2021.107090
30. Liang Q, Bao X, Sun Q et al (2020) Imaging VOC distribution in cities and tracing VOC emission sources with a novel mobile proton transfer reaction mass spectrometer. Environ Pollut 265:114628. https://doi.org/10.1016/j.envpol.2020.114628
31. Zhang QL, Zou X, Liang Q et al (2018) Development of dipolar proton transfer reaction mass spectrometer for real-time monitoring of volatile organic compounds in ambient air. Chin J Anal Chem 46:471–478. https://doi.org/10.1016/S1872-2040(17)61078-8
32. Shi W, Huo X, Tian Y et al (2021) Development of membrane inlet photoionization ion trap mass spectrometer for trace VOCs analysis. Talanta 230:122352. https://doi.org/10.1016/j.talanta.2021.122352
33. Wan E, Sun Z, Liu Y (2021) Real-time in situ detection and source tracing of different soot. Optik (Stuttg) 245:167711. https://doi.org/10.1016/j.ijleo.2021.167711
34. Zhang Q, Liu Y, Chen Y et al (2020) Online detection of halogen atoms in atmospheric VOCs by the LIBS-SPAMS technique. Opt Express 28:22844. https://doi.org/10.1364/oe.400324
35. Qu Y, Zhang Q, Yin W et al (2020) Real-time in situ detection of the local air pollution with laser-induced breakdown spectroscopy: errata. Opt Express 28:18750. https://doi.org/10.1364/oe.399360
36. Zhang Y, Zhang T, Li H (2021) Application of laser-induced breakdown spectroscopy (LIBS) in environmental monitoring. Spectrochim Acta Part B At Spectrosc 181:106218. https://doi.org/10.1016/j.sab.2021.106218
37. Mosier-Boss PA, Lieberman SH (2003) Detection of volatile organic compounds using surface enhanced Raman spectroscopy substrates mounted on a thermoelectric cooler. Anal Chim Acta 488:15–23. https://doi.org/10.1016/S0003-2670(03)00676-7
38. Sun WQ, Zhang Y, Fang SX (2019) Application of vacuum ultraviolet single-photon ionization mass spectrometer in online analysis of volatile organic compounds. Chin J Anal Chem 47:976–984. https://doi.org/10.1016/S1872-2040(19)61170-9
39. Bin TG, Gao W, Huang ZX et al (2011) Vacuum ultraviolet single-photon ionization time-of-flight mass spectrometer. Fenxi Huaxue/ Chin J Anal Chem 39:1470–1475. https://doi.org/10.1016/S1872-2040(10)60473-2
40. Czech H, Sippula O, Kortelainen M et al (2016) On-line analysis of organic emissions from residential wood combustion with single-photon

ionisation time-of-flight mass spectrometry (SPI-TOFMS). Fuel 177:334–342. https://doi.org/10.1016/j.fuel.2016.03.036
41. Wu C, Liu W, Jiang J et al (2019) An in-source helical membrane inlet single photon ionization time-of-flight mass spectrometer for automatic monitoring of trace VOCs in water. Talanta 192:46–51. https://doi.org/10.1016/j.talanta.2018.09.013
42. Huang Y, Li J, Tang B et al (2015) Development of a portable single photon ionization-photoelectron ionization time-of-flight mass spectrometer. Int J Anal Chem. https://doi.org/10.1155/2015/581696
43. Dodonov AF, Kozlovski VI, Soulimenkov IV et al (2000) High-resolution electrospray ionization orthogonal-injection time-of-flight mass spectrometer. Eur J Mass Spectrom 6:481–490. https://doi.org/10.1255/ejms.378
44. Zhang T, Zhou W, Jin W et al (2013) Direct desorption/ionization of analytes by microwave plasma torch for ambient mass spectrometric analysis. J Mass Spectrom 48:669–676. https://doi.org/10.1002/jms.3212
45. Guo H, Cheng HR, Ling ZH et al (2011) Which emission sources are responsible for the volatile organic compounds in the atmosphere of Pearl River Delta? J Hazard Mater 188:116–124. https://doi.org/10.1016/j.jhazmat.2011.01.081
46. Hui L, Liu X, Tan Q et al (2018) Characteristics, source apportionment and contribution of VOCs to ozone formation in Wuhan, Central China. Atmos Environ 192:55–71. https://doi.org/10.1016/j.atmosenv.2018.08.042
47. Liu B, Yang J, Yuan J et al (2017) Source apportionment of atmospheric pollutants based on the online data by using PMF and ME2 models at a megacity, China. Atmos Res 185:22–31. https://doi.org/10.1016/j.atmosres.2016.10.023
48. Zhu H, Wang H, Jing S et al (2018) Characteristics and sources of atmospheric volatile organic compounds (VOCs) along the mid-lower Yangtze River in China. Atmos Environ 190:232–240. https://doi.org/10.1016/j.atmosenv.2018.07.026
49. Song C, Liu B, Dai Q et al (2019) Temperature dependence and source apportionment of volatile organic compounds (VOCs) at an urban site on the north China plain. Atmos Environ 207:167–181. https://doi.org/10.1016/j.atmosenv.2019.03.030
50. Althuluth M, Mota-Martinez MT, Berrouk A et al (2014) Removal of small hydrocarbons (ethane, propane, butane) from natural gas streams using the ionic liquid 1-ethyl-3 -methylimidazolium tris(pentafluoroethyl) trifluorophosphate. J Supercrit Fluids 90:65–72. https://doi.org/10.1016/j.supflu.2014.02.006
51. Ovejero G, Romero MD, Díez E et al (2009) Thermodynamic modeling and simulation of styrene–butadiene rubbers (SBR) solvent equilibrium staged processes. Ind Eng Chem Res. https://doi.org/10.1021/ie9006497
52. Borbon A, Locoge N, Veillerot M et al (2002) Characterisation of NMHCs in a French urban atmosphere: overview of the main sources. Sci Total Environ 292:177–191. https://doi.org/10.1016/S0048-9697(01)01106-8
53. Mayo FR (1961) The dimerization of styrene1. 1289–1295.
54. Seila RL, Main HH, Arriaga JL et al (2001) Atmospheric volatile organic compound measurements during the 1996 Paso del Norte Ozone Study. Sci Total Environ 276:153–169. https://doi.org/10.1016/S0048-9697(01)00777-X
55. Blake DR, Smith TW, Chen T-Y et al (1994) Effects of biomass burning on summertime nonmethane hydrocarbon concentrations in the Canadian wetlands. J Geophys Res 99:1699. https://doi.org/10.1029/93jd02598
56. Guo H, Zou SC, Tsai WY et al (2011) Emission characteristics of nonmethane hydrocarbons from private cars and taxis at different driving speeds in Hong Kong. Atmos Environ 45:2711–2721. https://doi.org/10.1016/j.atmosenv.2011.02.053
57. Liu Y, Shao M, Lu S et al (2008) Source apportionment of ambient volatile organic compounds in the Pearl River Delta, China: Part II. Atmos Environ 42:6261–6274. https://doi.org/10.1016/j.atmosenv.2008.02.027
58. Wang T, Xia Z, Wu M et al (2017) Pollution characteristics, sources and lung cancer risk of atmospheric polycyclic aromatic hydrocarbons in a new urban district of Nanjing, China. J Environ Sci (China) 55:118–128. https://doi.org/10.1016/j.jes.2016.06.025
59. Li L, Xie S, Zeng L et al (2015) Characteristics of volatile organic compounds and their role in ground-level ozone formation in the Beijing-Tianjin-Hebei region, China. Atmos Environ 113:247–254. https://doi.org/10.1016/j.atmosenv.2015.05.021
60. Yan X, Xu L, Shi B et al (2020) Epidemiology and risk factors of chronic obstructive pulmonary disease in Suzhou: a population-based cross-sectional study. J Thorac Dis 12:5347–5356. https://doi.org/10.21037/jtd-20-1616
61. Xu Z, Huang X, Nie W et al (2017) Influence of synoptic condition and holiday effects on VOCs and ozone production in the Yangtze River Delta region, China. Atmos Environ 168:112–124. https://doi.org/10.1016/j.atmosenv.2017.08.035
62. Cheng HR, Saunders SM, Guo H et al (2013) Photochemical trajectory modeling of ozone concentrations in Hong Kong. Environ Pollut 180:101–110. https://doi.org/10.1016/j.envpol.2013.04.039
63. Cai C, Geng F, Tie X et al (2010) Characteristics and source apportionment of VOCs measured in Shanghai, China. Atmos Environ 44:5005–5014. https://doi.org/10.1016/j.atmosenv.2010.07.059
64. Ravina M, Panepinto D, Mejia Estrada J et al (2020) Integrated model for estimating odor emissions from civil wastewater treatment plants. Environ Sci Pollut Res 27:3992–4007. https://doi.org/10.1007/s11356-019-06939-5
65. Carter WPL (1994) Development of ozone reactivity scales for volatile organic compounds. Air Waste 44:881–899. https://doi.org/10.1080/1073161X.1994.10467290
66. Rappenglück B, Fabian P (1999) Nonmethane hydrocarbons (NMHC) in the Greater Munich Area/Germany. Atmos Environ 33:3843–3857. https://doi.org/10.1016/S1352-2310(98)00394-X
67. Na K, Kim YP, Moon KC (2003) Diurnal characteristics of volatile organic compounds in the Seoul atmosphere. Atmos Environ 37:733–742. https://doi.org/10.1016/S1352-2310(02)00956-1
68. Venecek MA, Carter WPL, Kleeman MJ (2018) Updating the SAPRC maximum incremental reactivity (MIR) scale for the United States from 1988 to 2010. J Air Waste Manag Assoc 68:1301–1316. https://doi.org/10.1080/10962247.2018.1498410
69. Geng F, Tie X, Xu J et al (2008) Characterizations of ozone, NOx, and VOCs measured in Shanghai, China. Atmos Environ 42:6873–6883. https://doi.org/10.1016/j.atmosenv.2008.05.045
70. Jenkin ME (2004) Analysis of sources and partitioning of oxidant in the UK - Part 1: the NO X-dependence of annual mean concentrations of nitrogen dioxide and ozone. Atmos Environ 38:5117–5129. https://doi.org/10.1016/j.atmosenv.2004.05.056
71. Boersma KF, Jacob DJ, Trainic M et al (2009) Validation of urban NO2 concentrations and their diurnal and seasonal variations observed from the SCIAMACHY and OMI sensors using in situ surface measurements in Israeli cities. Atmos Chem Phys 9:3867–3879. https://doi.org/10.5194/acp-9-3867-2009
72. Ionov DV, Timofeyev YM, Sinyakov VP et al (2008) Ground-based validation of EOS-Aura OMI NO2 vertical column data in the midlatitude mountain ranges of Tien Shan (Kyrgyzstan) and Alps (France). J Geophys Res Atmos 113:1–14. https://doi.org/10.1029/2007JD008659

Publisher's Note